Performance measurement of IEEE 802.11b-based networks affected by narrowband interference through cross-layer measurements

L. Angrisani, A. Pescapè, G. Ventre and M. Vadursi

Abstract: Researches and development efforts in wireless networking and systems are progressing at an incredible rate. Among them, measurement and analysis of performance achieved at network layer and perceived by end users is an important task. In particular, recent advances concerning IEEE 802.11b-based networks seem to be focused on the measurement of key parameters at different protocol levels in a cross-layered fashion, because of their inherent vulnerability to in-channel interference. By adopting a cross-layer approach on a real network set-up operating in a suitable experimental testbed, packet loss against signal-to-interference ratio in IEEE 802.11b-based networks is hereinafter assessed. Results of several measurements aimed at establishing the sensitivity of IEEE 802.11b carrier sensing mechanisms to continuous interfering signals and evaluating the effects of triggered interference on packet transmission.

1 Introduction

Performance measurement is a crucial task in the process of designing and validating new and complex communication network systems. In heterogeneous wireless scenarios, perceived performance is influenced by several characteristics typical of underlying wireless network layers, such as modulation schemes, framing procedures and stationary channel characteristics. Also, for any network scenario, actual quality of service (QoS) depends on the physical signal integrity. While such integrity can be kept under control in wired networks by wise network design and implementation, wireless channels are intrinsically subject to interference phenomena that cannot be directly controlled. In wired networks, in fact, the possible end-to-end QoS degradation is basically because of either the limited access to medium resources made available to each user or congestion phenomena, that can be caused by the simultaneous presence of several active users on the same network. On the contrary, signal integrity in IEEE 802.11b wireless local area networks (WLANs) can be strongly degraded by interferences from devices of different nature sharing the same band [1–3]. Since IEEE 802.11b WLANs exploit the unlicensed industrial scientific medical (ISM) band, electromagnetic interference comes out to be the most challenging issue in their design and performance evaluation [4]. With regard to IEEE 802.11b networks, it would therefore be very useful to evaluate how in-channel interference degrades network QoS. An approach not limited to just one protocol layer but consisting of joint physical and higher layer measurements is consequently desirable.

With the term 'cross-layer measurement', we mean a new approach consisting of appropriate measurements carried out, at the same time, at both application/transport layers and data link/physical layers and a proper analysis of the obtained results.

This work is a first attempt to put into relation the values of physical layer quantities, such as signal-to-interference ratio, and higher level parameters of interest, estimated in the same time interval. It presents an experimental study conducted in a semi-anechoic chamber in order to evaluate the effects of controlled in-channel interference on the performance of an IEEE 802.11b-based network. More specifically, the study moves along three directions. First, the sensitivity of IEEE 802.11b carrier sensing mechanism to continuous sinusoidal interference is verified. Then, possible packet corruption because of triggered bursty interference is evaluated. Finally, the relationship between a significant figure of merit at higher layers (packet loss ratio) and an important indicator of the quality of communication at physical layer (signal-to-interference ratio) in the presence of bursty sinusoidal in-channel interference is investigated. The rationale for the chosen types of interference sources is the following. Continuous sinusoidal signals are representative of possible spurious harmonics generated by common radiofrequency (RF) sources characterised by a bandwidth much narrower than that peculiar to Wi-Fi signals, whereas bursty sinusoidal interference is a good model for narrowband time division multiple access (TDMA) interfering signals [5–10].

To carry out the experiments, an active measurement approach is adopted, which uses synthetic UDP traffic through distributed internet traffic generator (D-ITG) [11–12] whose architecture allows us to measure QoS parameters both at sender and at receiver sides. A suitable measurement station is set up to the purpose.

The rest of the paper is organised as follows: Section 2 presents the motivation at the basis of the work, along with some proposals for wireless network performance

L. Angrisani, A. Pescapè and G. Ventre are with the Dipartimento di Informatica e Sistemistica, Università degli Studi di Napoli Federico II, Via Claudio, 21 – 80125, Napoli, Italy

M. Vadursi is with the Dipartimento per le Tecnologie, Università degli Studi di Napoli "Parthenope", Centro Direzionale di Napoli, Isola C4–80143, Napoli, Italy

E-mail: pescape@unina.it

assessment already presented in the literature. Section 3 gives details regarding the proposed measurement station and procedure. Section 4 describes the experimental activity conducted, and provides a proper analysis of the results, related to the effects of continuous sinusoidal interferences on carrier sensing, packet corruption because of bursty interference triggered on transmission and packet loss ratio in the presence of both periodic and random bursty interference. Finally, conclusions are drawn in Section 5, along with issues for ongoing and future research activities.

2 Motivations and related work

The term cross-layer networking means that the knowledge of the physical and medium access control (MAC) layers of the wireless medium is shared with higher layers and used to implement efficient methods for the allocation of network resources and applications over wireless scenarios [13]. Cross-layer protocol optimisation seems to be a fast growing research area within this context, which brings together researchers from physical to application layers [14]. All these efforts can be correctly finalised only with a clear and proper understanding of the performance at the different levels of the protocol stack and how they are correlated. Indeed, we are moving towards a framework which can simply highlight the mutual influence among the various layers of the protocol stack.

The aim of the proposed approach is to understand the behaviour of IEEE 802.11b-based networks at both transport and physical layers, and to gain a useful correlation between the values assumed by high-level QoS parameters and those by physical layer quantities. Such characterisation can be of great help both in the design and maintenance stage of an IEEE 802.11b network. At the earliest stages of the design of a WLAN indeed, physical measurements can be done to characterise the environment; from the achieved results, then, WLAN characteristics can be optimally tailored to meet the QoS requirements. Once the WLAN is operative, physical layer measures can be profitably exploited to infer possible causes of QoS degradation, when the latter is experienced at higher layers, or vice versa.

While a number of works on IEEE 802.11b performance evaluation [15−18] and interference between Bluetooth and IEEE 802.11b networks [19−27] are present in the literature; to the best of our knowledge, few works deal with cross-layer measurement of the performance of real wireless systems based on IEEE 802.11b protocol. According to the given definition of cross-layer measurement, our contribution aims at reducing this gap.

As for novel approaches to performance evaluation of IEEE 802.11b networks, a cross-layer analytical approach is presented in [28] and [29], which is addressed to applications running over wireless IP channels, based on a propagation model. The authors suggest that the proposed model should be used in classical queuing theory. In [30], the authors show that a physical layer model, optimal from a physical-centric point of view, results in a bad performance when used with a real protocol stack on the top of it. More precisely, it provides results in the case of WLANs with TCP traffic. In [31], the authors propose some simulation techniques to study the performance of wireless systems. They call these new simulation techniques cross-layer simulations because the generic proposed cross-layer network model, together with cross-layer simulation model facilities offered, should allow studies on cross-layer systems. Finally, the results of bit error measurements executed by an IEEE 802.11 compliant radio modem in an industrial environment are given in [32], along with some considerations for the design of MAC and link-layer protocols.

As already mentioned, the works in the field of performance evaluation of IEEE 802.11b networks show that the research is usually conducted theoritically or analytically. When it is performed through experiments over real network test beds, measurements are done only at a single layer.

Regarding approaches studying the interference on IEEE 802.11b networks, a lot of literature has been published on both coexistence between Bluetooth and IEEE 802.11b networks and related problems and optimisations. The work presented in [1] provides an introduction to coexistence issues between IEEE 802.11b and Bluetooth, showing that, although performance of both systems can degrade when they are collocated near enough, a number of techniques can be employed to virtually eliminate such issues. Unfortunately, a real assessment – using cross-layer measurements – to demonstrate this statement is missed. To pursue the target of providing a quantitative measure of the effects of mutual interference, a number of analytical studies are present in the literature. In [21], an analytical model for capturing the performance impact of Bluetooth interference on the collocated IEEE 802.11b is proposed. The analysis comprises interference at both physical and MAC layers of the IEEE 802.11b networks. In [22], an analytical model of the interference that 802.11 networks may experience, either because of a voice or because of a data Bluetooth link, is presented. In [33], the performance of IEEE 802.11b network is evaluated, in the presence of Bluetooth piconets, using a probabilistic approach. The analysis is described at both physical and MAC layers, and packet error rate and throughput of the IEEE 802.11b network are measured. As for simulation approaches, a simulation environment for modelling interference, based on detailed MAC and physical layers models, is presented in [26] and [27]. Finally, as for empirical studies, some experimental results (validating specific analytical models) are presented in [19] and [25] to show the effects of IEEE 802.11b and Bluetooth interference, and some results related to packet loss in IEEE 802.11b networks in the presence of Bluetooth are shown in [20]. The works presented in [23] and [24] report some preliminary results on performance in the presence of collocated IEEE 802.11b and Bluetooth networks.

To conclude this review, despite the number of studies dealing with interference analysis between Bluetooth and IEEE 802.11b, to the best of our knowledge, there is no previous literature focusing on cross-layer measurement in controlled environments like a semi-anechoic chamber. This approach permits (i) to link higher layer performance with lower layer and, at the same time, (ii) to clearly control unwanted interference. Therefore the proposed approach extends the results present in literature in that:

- an experimental approach is adopted, which takes into account real test signals in a controlled environment such as a semi-anechoic chamber (interfering signals, which can affect signal integrity, can thus be controlled and introduced according to the need);
- the approach follows a cross-layer assessment – through measurements over real networks – where transport and physical layer performance are measured and studied in a combined fashion;
- the proposed approach is applied to the study of packet loss ratio in the presence of controlled interference and more precisely:

- to measure the effects of continuous sinusoidal interference on carrier sensing, and the packet corruption as a result of bursty interference triggered on transmission;
- to measure the packet loss ratio in the presence of both periodic bursty and random bursty interference.

3 Measurement scenario

Experimental tests have been carried out in the semi-anechoic chamber at the Department of Electrical Engineering at the University of Napoli Federico II. In such environment, a total control of interference is, in fact, possible. The only interfering signal that is present on the communication channel is emitted from a signal generator suitably commanded, whereas possible uncontrolled interferences outside the chamber cannot affect the communication.

Fig.1 sketches the measurement station set up. It consists of (i) three hosts (two communicating hosts and one processing and control unit), (ii) an 802.11 access point (AP) D-link DI-624 +, (iii) a signal generator Rhode&Schwarz SML03 (9 kHz–3.3 GHz frequency range, with pulse modulation capability) acting as interference generator, (iv) an arbitrary waveform generator (AWG) Agilent Technologies 33120A (15 MHz maximum frequency), (v) a microwave horn antenna Amplifier Research AT4002A (0.8–5 GHz frequency range), (vi) an omnidirectional antenna EM-6865 (2–18 GHz frequency range, 10.16 cm diameter) called Probing antenna, (vii) a spectrum analyser Anritsu MS2687B (9 kHz–30 GHz input frequency range, up to 20 MHz resolution bandwidth), (viii) a digital storage oscilloscope (DSO) Agilent Technologies 54833D (1 GHz bandwidth, 4 Gsample/s sampling frequency, 8.2 Msample memory depth) and (ix) an EIA-232 → TTL converter, which makes a pulse generated on the serial port of the sender host available as a trigger signal for both spectrum analyser and DSO. The dashed box in Fig. 1 encloses instruments that are inside the semi-anechoic chamber. The two generators, the spectrum analyser, DSO and one of the hosts, which is the processing and control unit of the measurement station, are all interconnected via an IEEE 488 standard interface bus.

The signal inside the chamber is captured by the omnidirectional antenna, which is connected through a coaxial cable to the spectrum analyser outside the chamber. Besides providing the spectral density function of the signal captured by the antenna, the spectrum analyser can be utilised in zero span mode to attain the evolution against time of the signal power envelope.

Moreover, it can act as a downconverter to its intermediate frequency (66 MHz); thanks to this feature, the DSO can acquire the evolution against time of the downconverted signal, whose significant spectral content is totally included inside the DSO bandwidth. Finally, the controlled interference is emitted by the signal generator, which is outside the semi-anechoic chamber and feeds the microwave horn antenna located inside. To emit bursty interferences, the pulse modulation capability of the signal generator is exploited, whereas AWG is used as trigger source. In particular, AWG is commanded to generate a square-wave signal, which can be frequency modulated.

A heterogeneous (wired/wireless) communication is set up between a pair of hosts, named as Host 1 and Host 2. In particular, Host 1 is connected via a wired 100 Mbps link to the AP, which is its default gateway. Wireless communications, following standard IEEE 802.11b, actually take place between AP and Host 2, which are inside the chamber. Host 1 and Host 2 are the sender and receiver (and viceversa) of the traffic generation platform. The measurement station is equipped with a tool, D-ITG, which is used for the generation of the testing traffic. Details on D-ITG can be found in [11] and in [12].

Despite the wide range of available traffic patterns and other supported features, to trace a first reference framework for the variables subject of our study, D-ITG has been used in this work to generate constant bit rate (CBR) traffic. More precisely, the CBR traffic profiles reported in Table 1 have been taken into consideration.

With respect to its previous version, to make possible the work described in this paper, D-ITG has been provided with a triggering feature, very useful to our aim. In particular, when the sender starts the transmission of each packet, a voltage pulse is generated on a certain pin of its serial port. As the serial port of the host and the input trigger port of the spectrum analyser and the DSO associate different voltage levels to the same logic levels, the D-ITG triggering feature cannot be profitably used as trigger signal for the electronic instrumentation, unless a proper level conversion is performed. An EIA 232 → TTL converter has been used to convert voltage levels typical of EIA 232 standard used on the serial port of the sender to voltage levels typical of TTL standard, used for the spectrum analyser's trigger input.
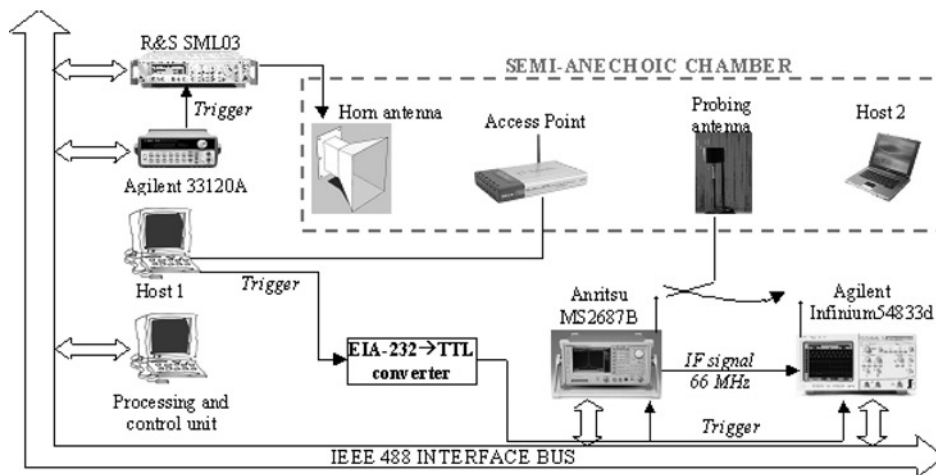

Fig. 1 *Measurement station*

Table 1: CBR traffic profiles

Packet size, bytes	Packet rate, pkt/s	CBR traffic profiles, Mpbs
1000	250	2
1000	750	6
1000	1000	8

4 Cross-layer measurements

The anechoic environment characterising our analysis is particularly suited to evaluate effects of interferences on the transmission. Interfering signals can, in fact, be properly controlled in such environment and the operator can easily modify them. Specifically, the signal generator utilised in the experiments is located outside the chamber and feeds the microwave horn antenna, which is located inside and provides for interference emission. Besides selecting the type of interfering signal, which can be either bursty or time continuous, and either unmodulated or modulated, eventually generated by exploiting arbitrary waveform generation capability, the operator can externally trigger the generator. Interfering signal can then be synchronised to packet transmission, so as to hit either packet header or payload, or even acknowledgement.

The signal evolution against time can be simply analysed through a DSO, provided that its bandwidth includes all the significant spectral component of the signal. IEEE 802.11b signals are located in the ISM band, at frequencies higher than 2.4 GHz. This poses a constraint on DSO choice, implying the utilisation of a modern and costly DSO characterised by 3 GHz bandwidth, at least. By exploiting the intermediate frequency (IF) output of the spectrum analyser, however, it is possible to use a less expensive, yet performing, DSO. In particular, the IF signal, which is the downconverted version of the signal captured by the antenna, is given as input to the DSO. As the IF signal is centred at a frequency much lower than 2.4 GHz, a common DSO characterised by 1-GHz bandwidth perfectly fits our needs. In the cases under examination, for instance, the IF signal is spectrally centered at 66 MHz. The signal downconverted at IF can be acquired and digitally processed, and measurement functionalities of the DSO, such as time interval measurement through cursors, can be exploited, according to the needs.

The external trigger to the signal generator can be exploited to verify the effects of interference at physical layer. As an example, Fig. 2 shows the DSO display when a single packet is generated and an interfering sinusoidal burst hits its payload, causing its re-transmission. Time interval T_{1-2} shown in Fig. 2, which is up to some hundreds of microseconds, is the time that elapses between the first packet transmission and its re-transmission. In the same figure, the arrow points the MAC layer acknowledgment, which is one shortest interframe spacing (SIFS) distant from the successful re-transmission. Signal analysis also helps analyse protocol robustness with respect to interfering bursts. As it is shown in Fig. 2, in fact, the packet is re-transmitted at a lower rate. Such mechanism is more evident in Fig. 3, which shows the DSO display when two packets are generated at application layer, and several interfering bursts of the same duration are emitted. In particular, the first packet is hit by interference and re-transmitted once (arrows A and B point at the interfered packet and the interference-free re-transmission, respectively), whereas the second packet (arrow C in the figure) is re-transmitted
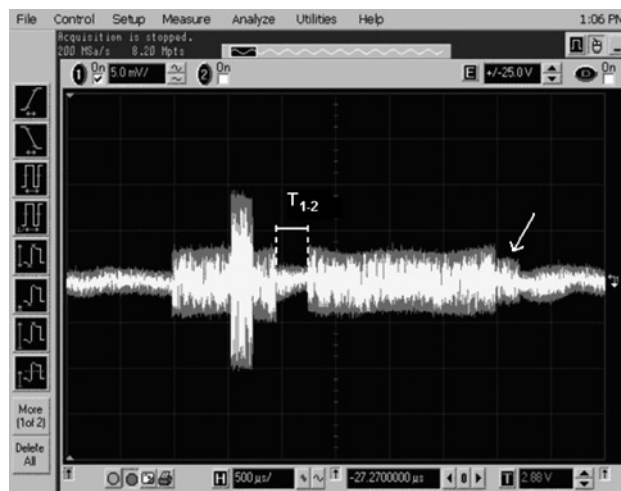

Fig. 2 *Single packet is hit by an interfering sinusoidal burst, re-transmitted and finally acknowledged*

several times and each re-transmission is hit by one or more interfering bursts. When transmission rate is lowered at 1 Mbps, packet transmission succeeds, although three interfering bursts hit the packet (they are pointed at by arrows D, E and F).

4.1 Effects of continuous sinusoidal interference on carrier sensing

Effects of interference occupying the channel before physical transmission can be analysed through the proposed measurement system. Owing to the carrier-sensing mechanism of IEEE 802.11b MAC protocol, when the interfering signal is sinusoidal and continuous, and therefore its power level P is practically constant over time, two situations may alternatively occur: either equipment that intends to transmit senses the channel, finds it continuously occupied (P is greater than a threshold value $P*$) and therefore does not transmit at all, or interference power level is too weak to consider the channel occupied, and therefore wireless transmission is unaffected. In practice, when the interfering power value is close to threshold value $P*$, successive carrier sensing operations do not provide the same result, that is after some trials the channel is usually considered free and the packet is transmitted. This is reasonably
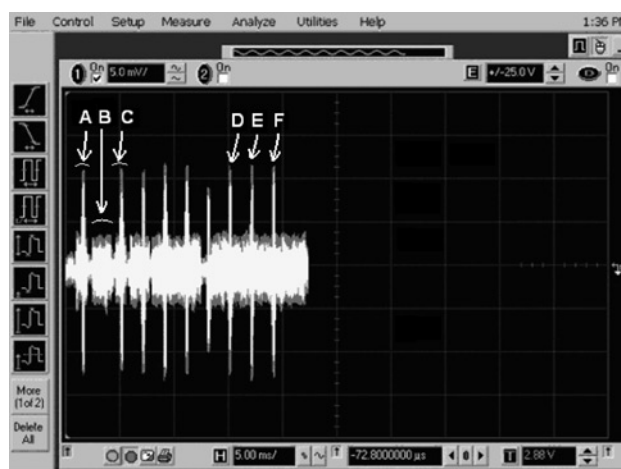

Fig. 3 *First packet is hit by an interfering sinusoidal burst, re-transmitted and finally acknowledged, and the second packet is hit and re-transmitted more than once*
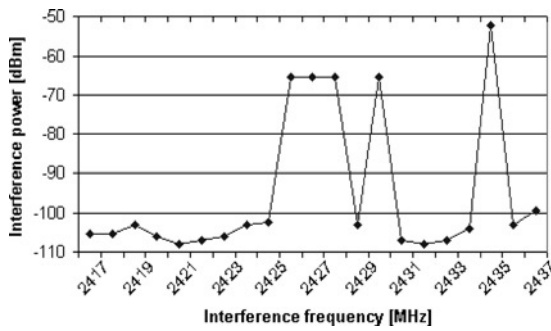
Fig. 4 *Power levels of sinusoidal interference causing a block in the 802.11b communication*

because of the limited sensitivity of the receiving apparatus that senses the channel.

Experiments carried out varying the frequency of sinusoidal interference have shown that the value of P^* depends on the frequency offset between the 802.11b carrier and the frequency of the sinusoidal interference. Fig. 4 shows the values of P^* obtained for different values of interference carrier frequency, when channel 4 (center frequency equal to 2.427 GHz) is used for wireless transmission. The values of P^* in the figure have been measured through the spectrum analyser's peak location capability over 100 repeated measurements, during which the 802.11b communication has been shut off.

What emerges is that the values of P^* can differ of even 56 dB. Similar results have been experienced when different channels have been chosen. Note that the absolute power levels given in Fig. 4 are dependent on the particular measurement scenario, that is AP, relative distance between hosts and instruments and so on, as different scenarios would be characterised by different threshold values.

Results reported in Fig. 4 could seem to be in contradiction to the expected robustness of the IEEE 802.11b direct sequence spread spectrum (DSSS) modulation with respect to narrowband interference. The proposed cross-layer approach allows to experimentally motivating such behaviour. When the generation of a continuous sinusoidal signal, characterised by power levels given in Fig. 4, is triggered after the packet transmission has begun, the interfering signal does not affect packet transmission at all (unless working in very disadvantageous conditions, that is SIR < -10 dB). Packets are, in fact, correctly received and acknowledged after an SIFS. On the contrary, the 100% packet loss ratio experienced when interference is not triggered, is not because severe packet corruption caused by interference, but is a consequence of the fact that transmission at physical layer does not begin at all.

4.2 Packet corruption because of bursty interference triggered on transmission

Besides being more realistic, bursty interference is hereinafter taken into consideration because continuous

interfering signals would block wireless transmission, as already remarked. In particular, a first set of experiments has been conducted to analyse packet corruption on single transmitted packets, when they are hit by a properly triggered interfering sinusoidal burst. As the system exhibits variable behaviour, depending on the frequency of interfering signal, different test frequencies have been analysed. Packet payload dimension has been fixed to 1000 byte, whereas interfering burst duration has been set to 200 μs. Whether a packet has been corrupted by interfering burst (and therefore re-transmitted), or not, it can be determined by a simple look at the DSO display. The DSO, in fact, is fed by the IF signal at the output of the spectrum analyser, which has been centred at 2.427 GHz, and set in zero span mode, maximum resolution bandwidth.

Table 2 gives the percentage values of corrupted packets, over 100 single transmissions, for three different frequencies and three different power levels of interfering signals. Please note that the power values in Table 2 represent power of continuous sinusoidal signals during the 'power on' state, and have been measured through the spectrum analyser, as explained in section 4.1. As expected, the probability that a packet is corrupted increases with interference power, although correlation between packet loss ratio and interference power is strongly dependent on interference frequency, as already experienced (Fig. 4).

4.3 Packet loss ratio in the presence of periodic bursty interference

As shown in the previous section, interference can be responsible for packet re-transmission. Depending on the packet rate, overflow on the packet queue at transmitter side, with consequent packet loss, can occur. Experiments presented in this section aim at highlighting the effects of sinusoidal interference on an important QoS parameter, such as packet loss ratio. Specifically, a cross-analysis of packet loss ratio and signal-to-interference ratio, measured at physical layer, is performed. Several scenarios, differentiated in terms of characteristics of the generated traffic and bursty interfering signal, are analysed.

As already pointed out, the transmission of a packet corrupted by interference and re-transmitted several times can succeed after a certain number of attempts. This is the reason why percentage values given in Table 2 do not have to be confused with packet loss ratios. In a strict sense, none of the packets corrupted by interference burst in the previous experiments is a lost packet, because related re-transmissions, not affected by interference, have succeeded. Indeed, packet re-transmission could indirectly be responsible for packet loss. When a packet is corrupted by interference and, consequently, not acknowledged, the queue at transmitter side can overflow as a result of re-transmissions, and packets can be irrecoverably lost.

Another set of experiments, with periodic bursty interference, has been carried out to investigate this issue. Wireless transmission during experiments has been kept active for

Table 2: **Percentage of corrupted packets over 100 single transmissions**

2422 MHz	Interference power, dBm	-47.5	-47.0	-46.0	-45.5	-45.0
	Corrupted packets, %	3	30	50	85	100
2427 MHz	Interference power, dBm	-50.8	-49.8	-49.3	-48.8	-47.3
	Corrupted packets, %	12	30	63	80	95
2432 MHz	Interference power, dBm	-43.3	-38.3	-33.3	-32.3	-31.3
	Corrupted packets, %	0	0	36	83	100

30 s; generated bursts duration has been made equal to 200 µs, whereas their rate, carrier frequency, and power have been varied. In particular, the same frequencies as in the previous experiments (reported in Table 2), and burst rates of 500 and 750 burst/s have been imposed; power level varies depending on frequency. A square wave, generated by the AWG, whose fundamental frequency is set equal to burst rate, has been utilised as external trigger to the interference generator. Table 3 reports the packet loss ratio as a function of interference power and burst rate, with regard to the considered interference frequencies and transmission rates. Table 3 is divided into three sub-tables, each of which accounts for a different frequency. For each burst power and rate, two values of packet loss ratio are given; the first refers to 250 pkts/s transmission rate, whereas the second, written in italics, refers to 750 pkts/s. The results show that for a given burst rate, power and carrier frequency, packet loss ratio increases with packet transmission rate. This is not unexpected, because the higher the transmission rate, the higher the number of lost packets when the queue at transmitter side overflows. Although in the great majority of the cases taken into consideration, the highest packet loss ratio is experienced as a result of the highest burst rate – given transmission rate and burst power and carrier frequency – there are cases in which, contrary to what could be expected, this does not happen. This can be explained by considering that bursts can also be emitted when no packet is being transmitted, and the fact that the queue at transmitter side is expected to be longer, on average, for higher burst rates does not imply that for limited observation intervals it necessarily overflows either more frequently or for longer time. Anyway, the expected correlation between interfering burst power and packet loss ratio has been experimentally verified.

Another interesting issue that experimental results put in evidence is that differences between minimum and maximum packet loss ratios is generally higher for 250 pkt/s than for 750 pkt/s transmission rate, given burst rate and frequency. In other words, decreasing interference power to reduce packet loss ratio is relatively more effective in case of slower transmission rates. Such experimental outcome is a further confirmation that communications characterised by high transmission rates are much more vulnerable to bursty interference, as lost packets are, in fact, lost because of queue overflowing.

4.4 Packet loss ratio in the presence of random bursty interference

The next step has consisted in dropping the hypothesis of periodic bursty interference, and conducting experiments in the presence of bursty interference characterised by random time occurrences. In particular, the frequency modulation capability of AWG has been exploited to produce a frequency-modulated square wave, which has been used as a trigger signal for the interference generator.

This set of measurements has been aimed at evaluating high-level performance of the system, measured through packet loss ratio, as a function of transmission rate, interfering signal duty cycle, average power and peak power. The following represent some definitions useful for the comprehension of the experimental tests we provided

- T_{On} = duration of a single burst of interference
- d (duty cycle) = T_{On}/T, where T is the average time interval between two successive bursts.
- S_{M} = power of the continuous interfering sinusoidal signal, hereinafter named peak power, measured through spectrum analyser.
- $S_{\mathrm{Burst}} = d \cdot S_{\mathrm{M}}$ = average power of interference.
- CP = channel power of IEEE 802.11b signal, measured through the spectrum analyser, in the absence of interference.
- SIR = signal-to-interference ratio = $\mathrm{CP}/S_{\mathrm{Burst}}$.

Channel power is measured through the spectrum analyser. It is worth noting that spectral analysis on IEEE 802.11b signals through a spectrum analyser places some constraints, because of the limited duration of transmitted packets. Transmission of long packets, in fact, requires no more than few milliseconds, and the minimum allowed sweep time covers several packets. In this case, because of IEEE 802.11b transmission protocol, even in the presence of high transmission rates, there would be time intervals between packets during which no signal is present in the channel, while the analyser is still sweeping the desired frequency span [34].

The spectrum analyser would then display something similar to what appears in Fig. 5, which can by no mean be considered the power spectrum of the transmitted signal. On the contrary, a synchronisation with transmitted packets would prevent from sweeping when no signal is

Table 3: Packet loss ratio in the presence of periodic bursty interference

| Frequency = 2.422 GHz				Frequency = 2.427 GHz				Frequency = 2.435 GHz			
Burst power,	Burst rate, burst/s			Burst power,	Burst rate, burst/s			Burst power,	Burst rate, burst/s		
dBm	500	750	1000	dBm	500	750	1000	dBm	500	750	1000
−44.0	0%	4.7%	0%	−46.8	0%	0%	32%	−31.3	0%	16%	51%
	49%	*66%*	*75%*		*47%*	*48%*	*78%*		*57%*	*71%*	*83%*
−43.0	0%	25%	0%	−46.3	0%	0%	38%	−30.8	12%	46%	62%
	59%	*75%*	*81%*		*51%*	*52%*	*80%*		*70%*	*82%*	*87%*
−42.5	0%	30%	45%	−45.8	0%	0%	45%	−30.3	39%	62%	72%
	65%	*77%*	*83%*		*58%*	*59%*	*83%*		*79%*	*89%*	*91%*
−41.5	19%	42%	57%	−45.3	0%	0%	48%	−29.3	68%	80%	82%
	74%	*82%*	*86%*		*63%*	*63%*	*84%*		*90%*	*93%*	*94%*
−41.0	29%	49%	61%	−44.3	14%	7.9%	57%	−28.8	78%	85%	86%
	78%	*84%*	*88%*		*74%*	*71%*	*86%*		*93%*	*95%*	*95%*
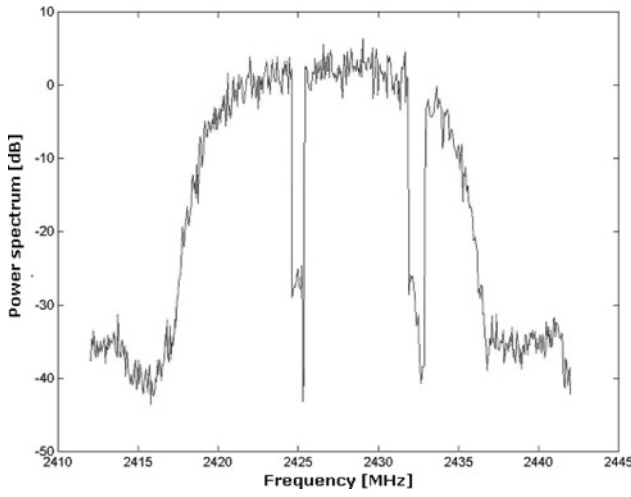
Fig. 5 *Power spectrum displayed by the spectrum analyser: sweep time longer than packet duration determines unreliable output*

present in the channel; signal power spectrum could therefore be reconstructed by joining power spectrum segments of successive packets. This solution is implemented by setting the spectrum analyser in gate mode, and performing the sweep over the selected frequency span at intervals synchronised with the transmission of packets; synchronisation is made possible by the EIA-232 → TTL converter that is used as a trigger signal for the spectrum analyser sweep. Although this technique has the disadvantage that measurement time grows inversely with packet transmission rate, it allows us to analyse signal power spectrum with the sensibility typical of a spectrum analyser, rather than performing an FFT-based analysis. Once the frequency span has been swept, and the power spectrum trace has been gained, channel power is measured by integrating the estimated

power spectrum, according to

$$CP = 10 \log_{10}\left[\frac{B_{ch}}{B_n} \left(\frac{1}{n_2 - n_1 + 1} \sum_{i=n_1}^{n_2} 10^{P_i/10} \right) \right] \quad (1)$$

where P_i is the ith power spectrum trace element, expressed in dBm, B_{ch} is the channel bandwidth, B_n is the equivalent noise bandwidth of the IF filter of the spectrum analyser and n_1 and n_2 are, respectively, the first and the last index of the power spectrum trace vector that limit the channel [35].

In this set of experiments, interfering signal carrier frequency has been fixed at 2.427 GHz, and packet loss ratio has been evaluated over 60-s transmission, in order to be able to confidently assume $S_{Burst} = d \cdot S_M$, on average. The idea is to study the dependence of system performance from the parameters of interference. This target implies a multidimensional analysis, as transmission rate has an important influence on packet loss ratio, and interference power (and therefore SIR) depends on duty cycle and peak power.

Tables 4, 5 and 6 report packet loss ratio for different interfering signal power levels and different transmission packet rates. They are related to duty cycle d equal to, respectively, 0.1, 0.15 and 0.2. All power values are given in dBm, whereas packet loss ratio is expressed in percentage relative terms.

Figs. 6 and 7 provide a three-dimensional diagram of packet loss ratio evolution as a function of transmission and interference parameters. Specifically, Fig. 6 shows packet loss ratio as a function of packet rate and SIR, for a given duty cycle ($d = 0.2$), whereas packet loss ratio in Fig. 7 is plotted in function of duty cycle and S_{Burst} for a packet rate equal to 750 pkt/s.

A more detailed representation of measurement results is shown Fig. 8 and 9, which provide evolution of packet loss ratio in function of, respectively, SIR (Fig. 8) and S_{Burst}

Table 4: PLR as a function of interference level, for different packet rates ($d = 0.1$)

		Interference power, dBm														
	S_M	-49.3	-46.2	-45.6	-44.1	-43.1	-42.1	-41.1	-40.2	-39.2	-38.2	-37.2	-34.1	-33.6	-33.1	-32.0
	S_{Burst}	-59.3	-56.2	-55.6	-54.1	-53.1	-52.1	-51.1	-50.2	-49.2	-48.2	-47.2	-44.1	-43.6	-43.1	-42.0
250 pkt/s	SIR	14.4	11.3	10.7	9.2	8.3	7.2	6.2	5.3	4.3	3.3	2.3	-0.8	-1.3	-1.8	-2.9
	PLR, %	2.7	4.1	6.3	24	30	31	35	38	35	35	36	38	37	34	32
750 pkt/s	SIR	14.2	11.1	10.5	9.0	8.0	7.0	6.0	5.1	4.1	3.1	2.1	-1.0	-1.5	-2.0	-3.1
	PLR, %	58	63	65	67	70	74	76	77	78	78	78	78	78	78	79
1000 pkt/s	SIR	14.7	11.6	11.0	9.5	8.5	7.5	6.5	5.6	4.6	3.6	2.6	-0.5	-1.0	-1.5	-2.6
	PLR, %	70	73	75	72	79	81	83	83	84	84	84	84	84	84	83

Table 5: PLR as a function of interference level, for different packet rates ($d = 0.15$).

		Interference power, dBm														
	S_M	-46.8	-45.9	-45.3	-43.8	-42.8	-41.9	-40.9	-39.9	-38.9	-37.9	-36.9	-33.9	-33.3	-32.8	-31.8
	S_{Burst}	-55.1	-54.4	-53.6	-52.1	-51.1	-50.1	-49.1	-48.2	-47.2	-46.2	-45.2	-42.1	-41.6	-41.1	-40.1
250 pkt/s	SIR	10.1	9.2	8.7	7.2	6.2	5.2	4.2	3.2	2.2	1.2	0.2	-2.8	-3.3	-3.9	-4.9
	PLR, %	7.8	34	38	48	50	55	56	53	57	58	56	55	54	57	57
750 pkt/s	SIR	9.9	9.0	8.5	7.0	6.0	5.0	4.0	3.1	2.1	1.1	0.1	-3.0	-3.5	-4.0	-5.1
	PLR, %	65	70	72	76	79	82	83	84	86	85	85	85	85	85	85
1000 pkt/s	SIR	10.5	9.6	9.0	7.5	6.5	5.5	4.5	3.6	2.6	1.6	0.6	-2.5	-3.0	-3.5	-4.5
	PLR, %	73	77	78	81	84	86	88	89	88	89	90	89	89	89	89

Table 6: PLR as a function of interference level, for different packet rates (d = 0.2)

	Interference power, dBm														
	S_M	−49.3	−46.3	−45.7	−44.2	−43.2	−42.2	−41.4	−40.7	−40.1	−39.5	−39.1	−34.2	−33.7	−33.2	−32.1
	S_{Burst}	−56.3	−53.3	−52.7	−51.2	−50.2	−49.2	−48.4	−47.7	−47.1	−46.5	−46.1	−41.2	−40.7	−40.2	−39.2
250 pkt/s	SIR	11.4	8.4	7.8	6.3	5.3	4.3	3.5	2.8	2.2	1.6	1.2	−3.7	−4.3	−4.7	−5.9
	PLR, %	12	19	27	33	39	44	54	61	64	63	64	65	66	64	65
750 pkt/s	SIR	11.2	8.2	7.6	6.1	5.1	4.1	3.3	2.6	2.0	1.4	1.0	−3.9	−4.4	−4.9	−6.0
	PLR, %	71	75	78	80	83	85	88	88	88	87	89	88	88	88	88
1000 pkt/s	SIR	11.7	8.7	8.1	6.6	5.6	4.6	3.8	3.1	2.5	1.9	1.5	−3.4	−3.9	−4.4	−5.5
	PLR, %	79	82	83	85	88	89	90	91	91	91	91	92	92	92	91

(Fig. 9), for different combinations of duty cycle and transmission packet rate. From the analysis of both three- and bi-dimensional plots, the following considerations can be drawn:

- Since channel power of IEEE 802.11b signal does not vary significantly with transmission rate, SIR and S_{Burst} are equivalent figures of merit, for our particular cases.
- All plots are characterised by a similar threshold-like evolution. A transition region can be singled out in all cases, which determines the separation between a region in which lower SIR (or higher S_{Burst}) result in a packet loss ratio increase, and a region in which maximum
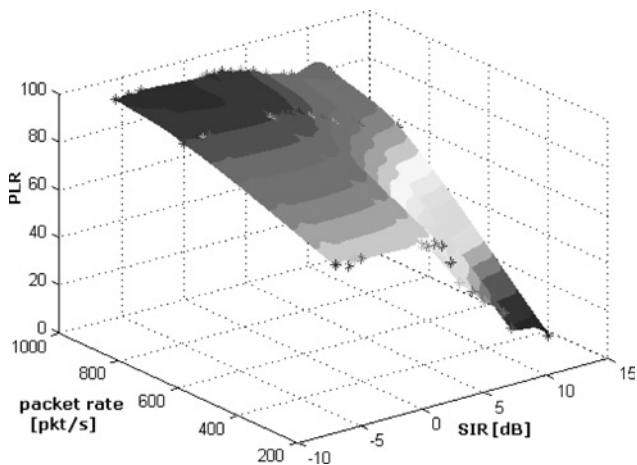

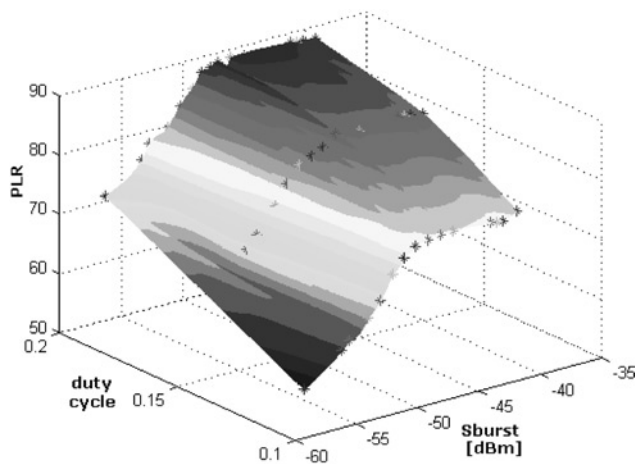**Fig. 6** *PLR as a function of packet rate and SIR (d = 0.2)*

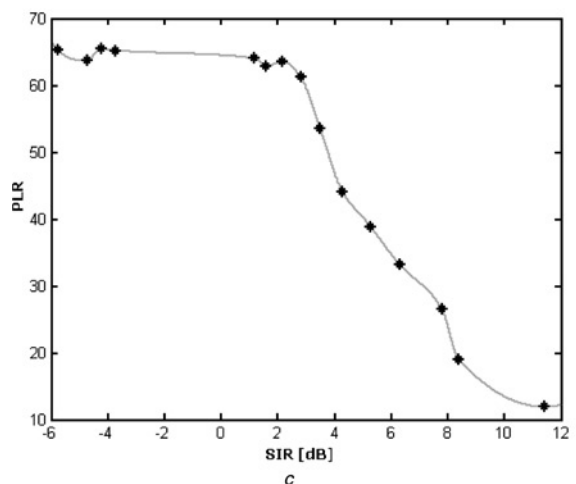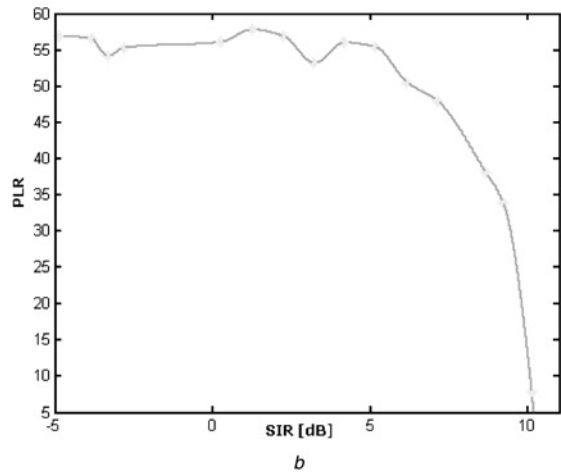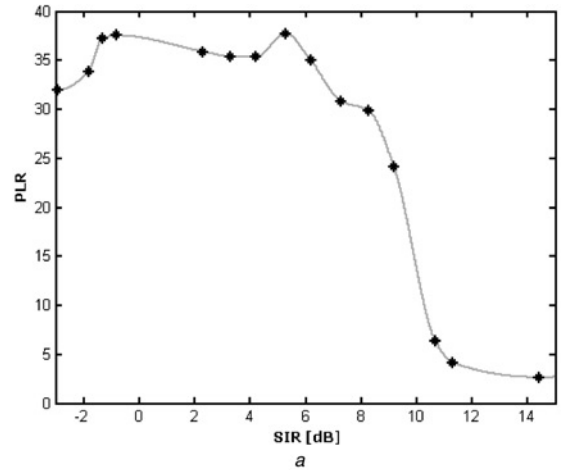**Fig. 7** *PLR as a function of d and S_{Burst} (packet rate = 750 pkt/s)*

Fig. 8 *Pocket loss ratio against SIR*
a Rate = 250 pkt/s; *d* = 0.1
b Rate = 250 pkt/s; *d* = 0.15
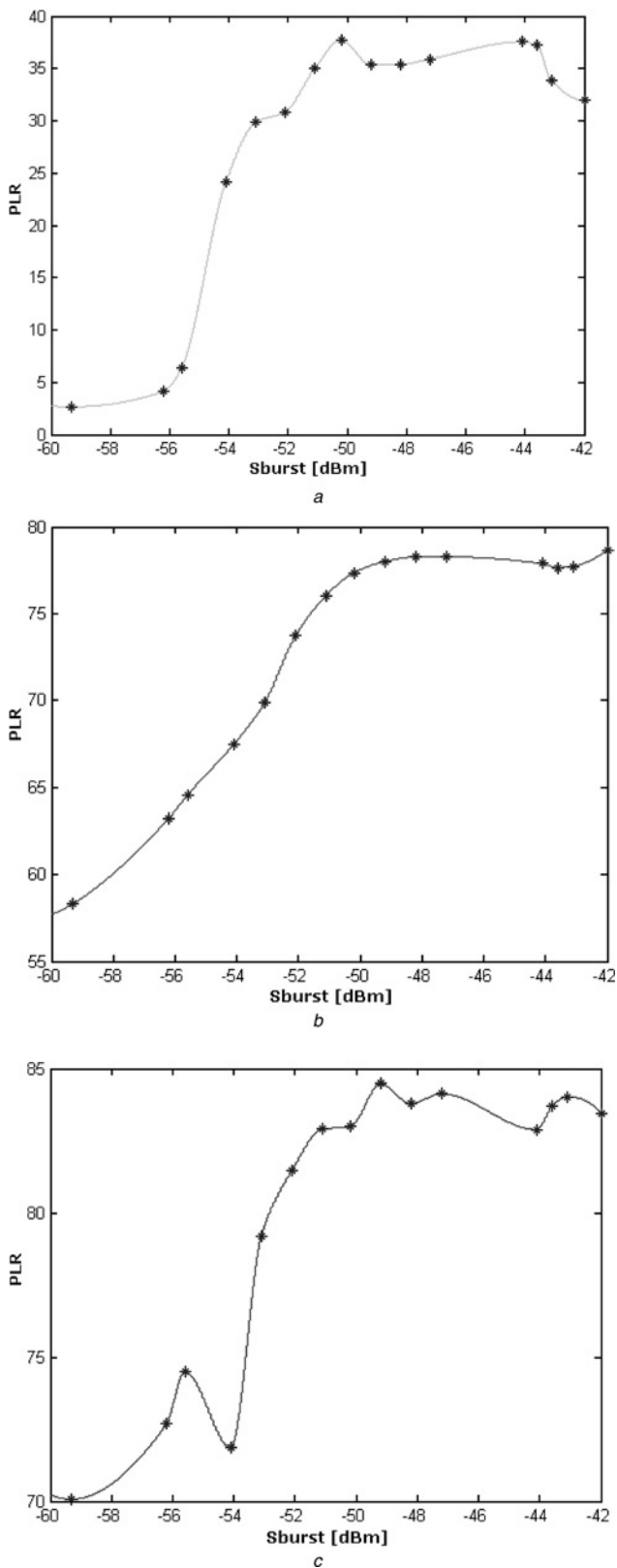*c* Rate = 250 pkt/s; *d* = 0.2

Fig. 9 *Pocket loss ratio against S_{Burst}*

a Rate = 250 pkt/s; *d* = 0.1
b Rate = 750 pkt/s; *d* = 0.1
c Rate = 1000 pkt/s; *d* = 0.1

packet loss ratio is reached; the same behaviour is experienced for all the packet rate, packet size and interference duty cycle taken into consideration.

• Maximum packet loss ratio is not necessarily equal to 100%, but depends on packet transmission rate and burst average frequency. In other words, given a certain burst

average frequency, once SIR has gone below a certain threshold, packet loss ratio is not affected by further SIR degradation, but rather depends on the mutual relation between signal and interference rate.

• Specifically, given the transmission rate, it is the interference burst rate that determines packet loss ratio maximum value, once SIR has gone below a certain value.

5 Conclusion

This paper has presented a cross-layer measurement approach to assess the performance of heterogeneous wired/wireless scenario, with particular regard to packet loss ratio evaluation.

To the best of our knowledge, our approach is one of the first attempts to analyse data provided by measurements carried out at different layers, taking into account real test-beds in an interference-controlled scenario.

The analysis of the results achieved through the proposed fully comprehensive approach has allowed the drawing of some relevant considerations. They can be summarised in the following points:

• physical signal integrity in IEEE 802.11b systems is not the main threat to packet loss ratio, as adopted modulation has proved very robust with respect to narrowband interference;
• the achieved results confirm that the IEEE 802.11b MAC protocol can strongly suffer from the presence of interference, as carrier sensing is very sensitive to that, and delayed transmissions can be responsible for queue overflow at transmitter side and are actually the cause of packet loss; a quantification of this phenomena in the considered scenario is provided;
• in the presence of bursty interference, for a given transmission rate and average burst rate, once SIR has gone below a certain threshold, packet loss ratio is not affected by further SIR degradation, but rather it depends on the mutual relation between signal and interference rate;
• given the transmission rate, it is the interference average burst rate that determines packet loss ratio maximum value, once SIR has gone below a certain value.

Future research activity will be oriented to vary characteristics of both interfering and 802.11b signals and to extend QoS parameters taken into consideration for a thorough performance evaluation.

6 Acknowledgments

7 References

1 Lansford, J., Stephens, A., and Nevo, R.: 'Wi-Fi (802.11b) and Bluetooth: enabling coexistence', *IEEE Netw.*, 2001, **15**, pp. 20–27
2 Golmie, N., Chevrollier, N., and Rebala, O.: 'Bluetooth and WLAN coexistence: challenges and solutions', *IEEE Wirel. Commun.*, 2003, **10**, (6), pp. 22–29
3 Matsumoto, Y., Takeuchi, M., Fujii, K., Sugiura, A., and Yamanaka, Y.: 'Performance analysis of interference problems involving DS-SS WLAN systems and microwave ovens', *IEEE Trans. Electromagn. Compat.*, 2005, **47**, (1), pp. 45–53
4 Takaya, K., Maeda, Y., and Kuwabara, N.: 'Experimental and theoretical evaluation of interference characteristics between

2.4-GHz ISM-band wireless LANs', Proc. IEEE Int. Symp. Electromagn. Compatibility, 24–28 August 1998, vol. 1, pp. 80–85

5 Agilent Technologies Literature: 'Agilent Technologies wireless test solutions', Application Note 5968-3578E, 2002

6 Agilent Technologies Literature: 'Understanding GSM/EDGE transmitter and receiver measurements for base transceiver stations and their components', Application Note 5968-2320E, 2002

7 Angrisani, L.: 'A wavelet packet transform-based approach for interference measurement in spread spectrum wireless communication systems', *IEEE Trans. Instrum. Measur.*, 2005, **54**, (6), pp. 2272–2280

8 Tektronix Literature: 'Fundamental of interference in mobile networks', Application Note 2GW-14 758-0, 2001

9 Worthen, A., and Stark, W.: 'Interference mitigation in frequency-hopped spread-spectrum systems'. Proc. IEEE 6th Symp. on Spread-Spectrum Tech. Appl., 6–8 September 2000, pp. 58–62

10 Amin, M.G.: 'Interference mitigation in spread spectrum communication systems using time–frequency distributions', *IEEE Trans. Signal Process.*, 1997, **45**, (1), pp. 90–101

11 http://www.grid.unina.it/software/ITG

12 Avallone, S., Emma, D., Pescapè, A., and Ventre, G.: 'High performance internet traffic generators', *J. Supercomput.*, 2006, **35**, pp. 5–26

13 Shakkottai, S., Rappaport, T.S., and Karlsson, P.C.: 'Cross-layer design for wireless networks', *IEEE Commun. Mag.*, 2003, **41**, (10), pp. 74–80

14 Chandramouli, R., Shorey, R., Srimani, P.K., Wang, X., and Yu, H.: 'Recent advances in wireless multimedia', *IEEE J. Sel. Areas Commun.*, 2003, **21**, (10), pp. 1501–1505

15 Singh, J.P., Bambos, N., Srinivasan, B., and Clawin, D.: 'Wireless LAN performance under varied stress conditions in vehicular traffic scenarios'. Proc. IEEE Vehicular Technology Conf., 2002, vol. 2, pp. 743–747

16 Messier, A., Robinson, J., and Pahlavan, K.: 'Performance monitoring of a wireless campus area network', *Proc. IEEE 2nd Annal Conf. Local Computer Networks.*, November 1997, pp. 232–238

17 Xylomenos, G., and Polyzos, G.C.: 'TCP and UDP performance over a wireless LAN'. Proc. INFOCOM 99, March 1999, vol. 2, pp. 439–446

18 Amaro, J.C., and Lopes, R.P.: 'Performance analysis of a wireless MAN'. Proc. IEEE Int. Symp. Network Computing and Applications, October 2001, pp. 358–361

19 Howitt, I., Mitter, V., and Gutierrez, J.: 'Empirical study for IEEE 802.11 and Bluetooth interoperability'. Proc. IEEE Vehicular Technology Conf., Spring 2001, vol. 2, pp. 1109–1113

20 Punnoose, R.J., Tseng, R.S., and Stancil, D.D.: 'Experimental results for interference between Bluetooth and IEEE 802.11b DSSS systems'. Proc. IEEE Vehicular Technology Conf., Fall 2001, vol. 1, pp. 67–71

21 Fainberg, M., and Goodman, D.: 'Analysis of the interference between IEEE 802.11b and Bluetooth systems'. Proc. IEEE Vehicular Technology Conf., Fall 2001, vol. 2, pp. 967–971

22 Chiasserini, C.F., and Rao, R.R.: 'Performance of IEEE 802.11 WLANs in a Bluetooth environment'. Proc. IEEE Wireless Communications and Networking Conf., 2000, vol. 1, pp. 94–99

23 Matheus, K., and Zurbes, S.: 'Co-existence of Bluetooth and IEEE 802.11b WLANs: results from a radio network testbed'. Proc. IEEE Intern. Symp. Personal, Indoor and Mobile Radio Communications 2002, 15–18 September 2002, vol. 1, pp. 151–155

24 Chandrashekhar, M.V.S., Choi, P., Maver, K., Sieber, R., and Pahlavan, K.: 'Evaluation of interference between IEEE 802.11b and Bluetooth in a typical office environment'. Proc. IEEE Intern. Symp. Personal, Indoor and Mobile Radio Communications, September 2001, vol. 1, D71–D75

25 Howitt, I.: 'Bluetooth performance in the presence of 802.11b WLAN', *IEEE Trans. Veh. Technol.*, 2002, **51**, (6), pp. 1640–1651

26 Golmie, N., Van Dyck, R.E., and Soltanian, A.: 'Interference of bluetooth and IEEE 802.11: simulation modeling and performance evaluation'. Proc. ACM Int. Workshop on Modeling, Analysis and Simulation of Wireless and Mobile Systems, 2001, pp. 11–18

27 Golmie, N., Van Dyck, R.E., Soltanian, A., Tonnerre, A., and Rébala, O.: 'Interference evaluation of bluetooth and IEEE 802.11b systems', *Wirel. Netw.*, 2003, **9**, (3), pp. 201–211

28 Moltchanov, D., Koucheryavy, Y., and Harju, J.: 'Cross-layer performance evaluation of IP-based applications running over the air interface'. Proc. NET-CON IFIP TC6'2004, Palma de Mallorca, Spain, November 2004

29 Moltchanov, D., Koucheryavy, Y., and Harju, J.: 'Cross-layer modeling of wireless channels for data-link and IP layer performance evaluation', *Comput. Commun.*, 2006, **29**, (7), pp. 827–841

30 Pollin, S., Bougard, B., Lenoir, G., Van Poucke, B., Van der Perre, L., Catthoor, F., and Moerman, I.: 'Cross-layer exploration of link adaptation in wireless LANs with TCP traffic'. IEEE Symp. Communications and Vehicular Technology, Eindhoven, The Netherlands, November 2003

31 Dhaou, R., Gauthier, V., Issoufou Tiado, M., Becker, M., and Beylot, A.L.: 'Cross layer simulation: application to performance modelling of networks composed of MANETs and satellites'. Tutorial at HET-NETs '04, 2nd Int. Working Conf. Performance Modelling and Evaluation of Heterogeneous Networks, July 2004

32 Willig, A., Kubisch, M., Hoene, C., and Wolisz, A.: 'Measurements of a wireless link in an industrial environment using an IEEE 802.11-compliant physical layer', *IEEE Trans. Ind. Electron.*, 2002, **49**, (6), pp. 1265–1282

33 Feng, W., Nallanathan, A., and Krishna, G.H.: 'Performance of physical (PHY) and medium access control (MAC) layers of IEEE 802.11b in the presence of bluetooth piconets'. IEEE Vehicular Technology Conf., Spring, April 2003, vol. 2, pp. 1489–1492

34 Agilent Technologies Literature: 'Optimizing spectrum analyzer measurement speed'. Application Note 5968-3411E, May 2000

35 Agilent Technologies Literature 'Spectrum analyzer measurements and noise'. Application Note 5966-4008E, February 2003